

Supplementary information

Experimental support for the model of Bray-Liebhafsky oscillatory reaction based on the heterogeneous effects

Itana Nuša Bujanja^a, Annette Fiona Taylor^b and Dragomir Stanisavljev^{a,*}

^aUniversity of Belgrade, Faculty of Physical Chemistry,
Studentski trg 12-16, 11158 Belgrade, Serbia

*Corresponding Author: dragisa@ffh.bg.ac.rs

^bThe University of Sheffield, Department of Chemical and Biological Engineering,
Mappin Street, Sheffield, S1 3JD, UK

As a natural consequence of a rippling mixture surface due to the mechanical mixing and oxygen escape through randomly leaving bubbles in all measurements of the gaseous-flow during the BL reaction a noise was present. Noise was removed through the Origin 8 application by applying a Savitzky-Golay filtering with 500 points of window, periodic boundary condition and 4th polynomial order Figure 1SI illustrates only a small part of the experimentally obtained gaseous-flow in time, in an experiment in which the stirring rate of the BL reaction mixture was 100 rpm, and the processed data with the Savitsky-Golay smoothing method.

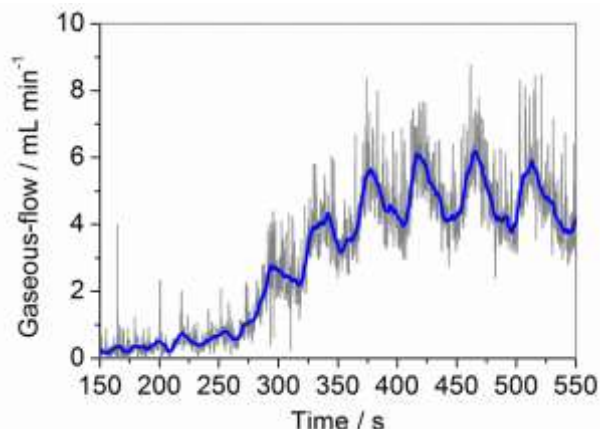


Figure 1SI. Illustrative comparison between experimentally obtained gaseous-flow in time (grey line) and gaseous-flow in time processed with Savitsky-Golay smoothing method (blue line). Data shown in this figure is obtained for the BL reaction under the following experimental conditions: $[\text{KIO}_3]_0=0.34$ M, $[\text{H}_2\text{SO}_4]_0=0.05$ M, $[\text{H}_2\text{O}_2]_0=0.33$ M, at $T=(60.0 \pm 0.3)$ °C and 100 rpm stirring rate.

In Figure 2 from the manuscript only one experiment obtained at particular stirring rate is shown in order to illustrate influence of mixing to Bray-Liebhafsky reaction dynamics. Experiments performed under stirring rates of 100 rpm and 1100 rpm were performed in 5 replicates. Figures 2SI and 3SI show oscillograms obtained by a potentiometric method, gaseous-flow vs time diagram (processed signal with the Savitsky-Golay smoothing method (blue or orange curve depending on stirring rate value)), as well as integrated signals of gaseous-flow vs time plots obtained from smoothed diagrams. Experiments which are illustratively shown in Figure 2 in manuscript text are encircled in both Figure 2SI and 3SI.

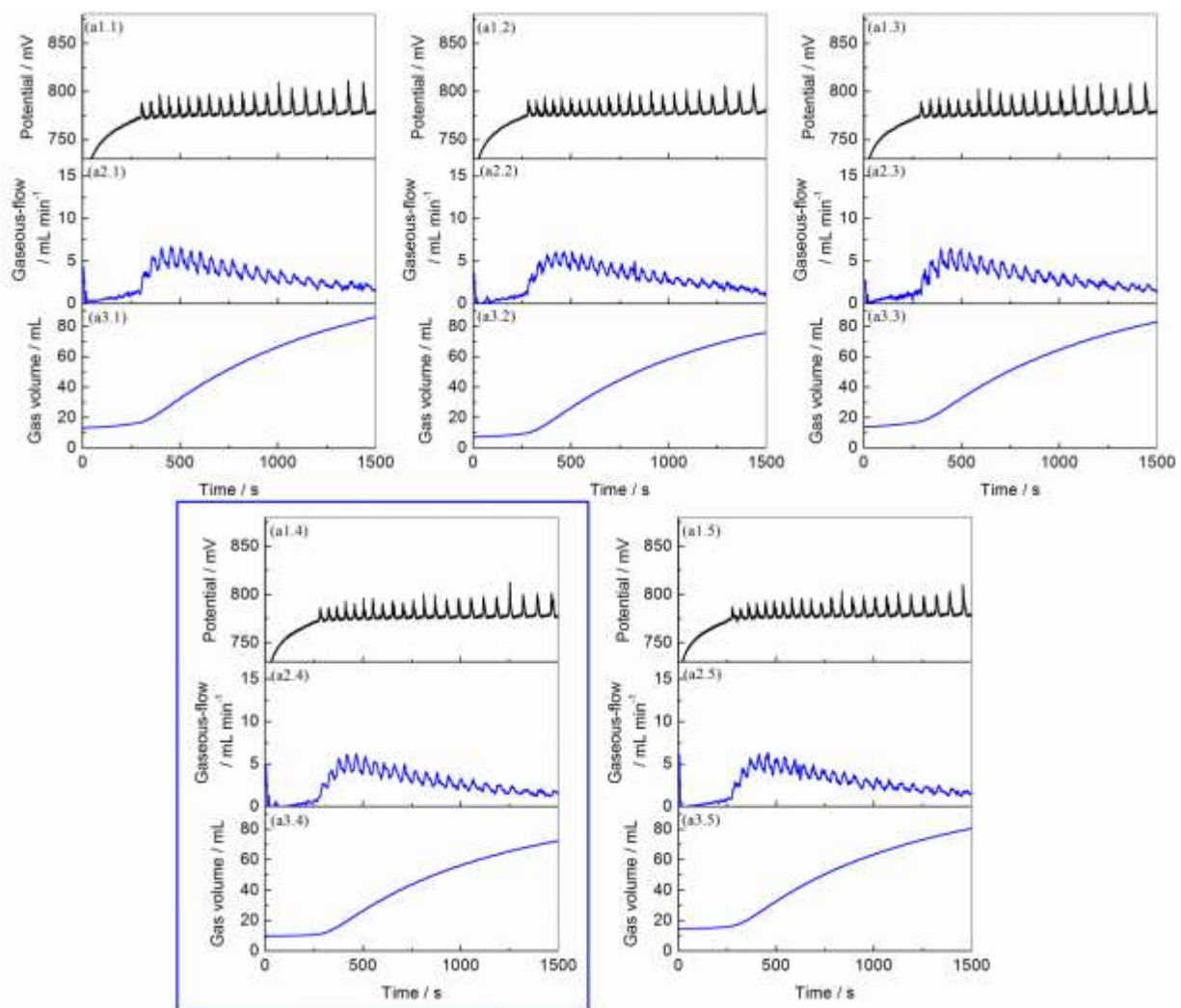


Figure 2SI. BL reaction dynamics obtained under 100 rpm stirring rate. Oscillograms shown on (a1.number of replicate) were obtained by a potentiometric method, while diagrams (a2.number of replicate) represents smoothed signal of gaseous-flow in time. Figures (a3.number of replicate) show integrated smoothed signals of gaseous-flow in time plots shown in (a2.number of replicate).

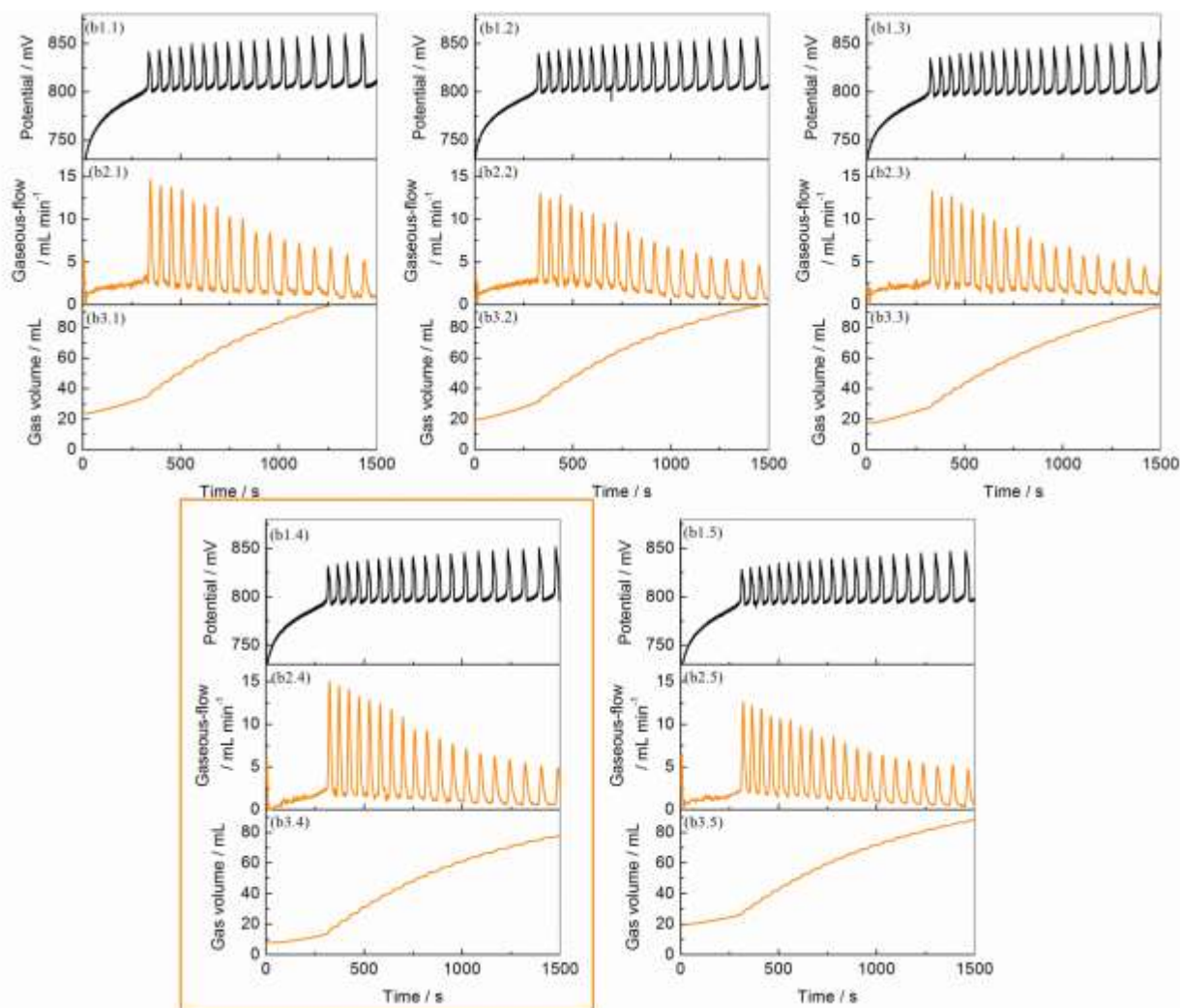


Figure 3SI. BL reaction dynamics obtained under 1100 rpm stirring rate. Oscillograms shown on (b1.number of replicate) were obtained by a potentiometric method, while diagrams (b2.number of replicate) represents smoothed signal of gaseous-flow in time. Figures (b3.number of replicate) show integrated smoothed signals of gaseous-flow in time plots shown in (b2.number of replicate).

In manuscript text, for both group of experiments performed under 100 and 1100 rpm, values of induction periods and number of oscillations during first 1500 s from H₂O₂ addition are shown with mean values and standard errors of the mean determined from 5 replicates. In this regard details are given in Table 1SI.

Table 1SI. Induction times and numbers of oscillations during first 1500 s of reaction are given per experimental replicate and per stirring rate.

Stirring rate / rpm	Experiment replicate	Induction time / s	Number of oscillations during first 1500 s
100	1	300,9	20
	2	281,46	22
	3	291,24	20
	4	281,46	22
	5	276,1	23
	Mean value	286,232	21,4
	Standard error of the mean	4,40699	0,6
1100	1	335,67	17
	2	324,92	18
	3	324,92	18,5
	4	314,79	19
	5	311,06	20
	Mean value	322,272	18,5
	Standard error of the mean	4,33139	0,5

In manuscript text Figure 4 is shown to illustrate that thermostat is not able to completely eliminate all thermal effects during oscillations. Temperature was satisfactorily kept constant up to ± 0.3 °C between different experiment replicates. Since temperature “jumps” in Figure 4 may be ascribed to a very fast evolution of heat during the iodine oxidation reaction, we calculated evolved heat during oscillation from 2nd, 3rd, 4th, 5th and 6th oscillation from one of the performed experiments (Figure 3(b1) from manuscript). In the manuscript calculation for the 2nd oscillation is illustratively shown and here more details are given.

2nd oscillation:

$$Q = m \cdot c \cdot \Delta T = 30 \text{ g} \cdot 4,186 \text{ Jg}^{-1}\text{K}^{-1} \cdot (59.93 - 59.74) \text{ K} = 23.9 \text{ J}$$

3rd oscillation:

$$Q = m \cdot c \cdot \Delta T = 30 \text{ g} \cdot 4,186 \text{ Jg}^{-1}\text{K}^{-1} \cdot (60.01 - 59.87) \text{ K} = 17.6 \text{ J}$$

4th oscillation:

$$Q = m \cdot c \cdot \Delta T = 30 \text{ g} \cdot 4,186 \text{ Jg}^{-1}\text{K}^{-1} \cdot (60.08 - 59.92) \text{ K} = 20.1 \text{ J}$$

5th oscillation:

$$Q = m \cdot c \cdot \Delta T = 30 \text{ g} \cdot 4,186 \text{ Jg}^{-1}\text{K}^{-1} \cdot (60.11 - 59.95) \text{ K} = 20.1 \text{ J}$$

6th oscillation:

$$Q = m \cdot c \cdot \Delta T = 30 \text{ g} \cdot 4,186 \text{ Jg}^{-1}\text{K}^{-1} \cdot (60.14 - 59.99) \text{ K} = 18.8 \text{ J}$$

From calculated data above, the mean value (20.1 J) and standard error of the mean (1,06 J) are determined.

Besides, in order to estimate the real evolved heat for the iodine oxidation in an oscillation we determined the iodine concentration at the base (before oscillation takes place) and maximum of the oscillation. For this purpose an Agilent UV/VIS spectrophotometer was used. Like it is explained in manuscript text every taken aliquot was diluted 4 times with deionized water previously kept on ice to slow down general kinetics and decrease unfavorable influence of bubbles during spectrophotometric measurements. Aliquots were taken from the 2nd to 6th oscillation, so change of the iodine amount during an oscillation is represented as the mean value from five oscillations with standard error of the mean. In Figure 4SI all recorded UV/VIS spectra of diluted aliquots are shown.

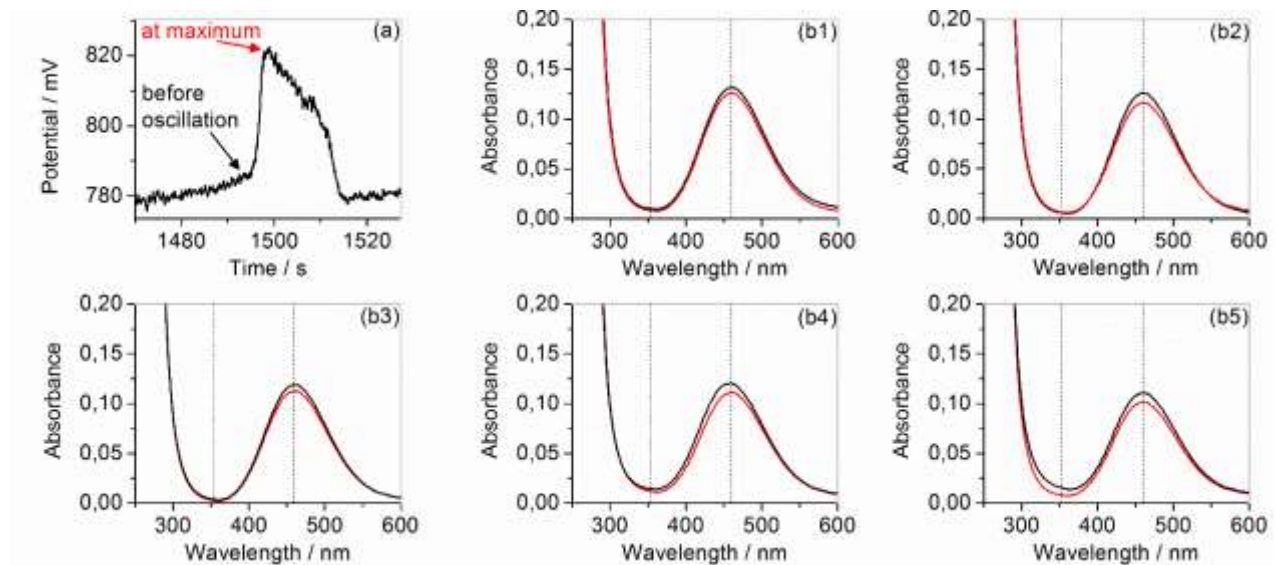


Figure 4SI. Enlarged part of oscillogram illustrating moment when aliquots are taken for UV/VIS measurements (a). UV/VIS spectra of aliquots taken before oscillation (black line) and at the oscillation maximum (red line) for 2nd (b1), 3rd (b2), 4th (b3), 5th (b4) and 6th (b5) oscillation.

From UV/VIS measurements concentrations of both components I_2 and I_3^- are determined by solving two equations:

$$A_{353} = \epsilon_{353}^{I_2} b[I_2] + \epsilon_{353}^{I_3^-} b[I_3^-]$$

$$A_{460} = \epsilon_{460}^{I_2} b[I_2] + \epsilon_{460}^{I_3^-} b[I_3^-]$$

while molar absorption coefficients for appropriate components at specific wavelengths are following: $\epsilon_{353}^{I_2} = 18 \text{ cm}^2 \text{ M}^{-1}$, $\epsilon_{353}^{I_3^-} = 26400 \text{ cm}^2 \text{ M}^{-1}$, $\epsilon_{460}^{I_2} = 746 \text{ cm}^2 \text{ M}^{-1}$ and $\epsilon_{460}^{I_3^-} = 975 \text{ cm}^2 \text{ M}^{-1}$, and length of the light path was $b = 1 \text{ cm}$.

Table 2SI summarizes values of absorbances and calculated values of:

- total iodine molar concentration **[Total iodine]** = $[I_2] + [I_3^-]$ (determined from diluted aliquots),

- total iodine molar concentration changes per oscillation $\Delta[\text{Total iodine}]$ (calculated as difference between total iodine molar concentration at oscillation maximum and total iodine molar concentration before oscillation, determined from diluted aliquots),
- total iodine molar concentration changes per oscillation $\Delta[\text{Total iodine}]_{\text{aliquot}}$ without dilution, (calculated as: $\Delta[\text{Total iodine}]_{\text{aliquot}} = 4 \cdot \Delta[\text{Total iodine}]$) and
- total iodine amount changes, in moles, per oscillation $\Delta n(\text{Total iodine})_{\text{in 30 mL reaction mixture}}$ without dilution and calculated for 30 mL of reaction solution (calculated as: $\Delta n(\text{Total iodine})_{\text{in 30 mL reaction mixture}} = \Delta[\text{Total iodine}]_{\text{aliquot}} \cdot 30 \text{ mL} / 1000 \text{ mL}$).

Table 2SI. Results from UV/VIS measurements of diluted aliquots taken from 2nd to 6th oscillation.

Oscillation number		2nd	3rd	4th	5th	6th
Absorbance at 460 nm	before oscillation	0.13167	0.12594	0.119	0.12027	0.1108
	at oscillation maximum	0.12588	0.11622	0.11294	0.11108	0.10166
Absorbance at 353 nm	before oscillation	0.00993	0.0056	0.00411	0.01455	0.0155
	at oscillation maximum	0.00812	0.00636	0.00298	0.01213	0.00805
$[\text{I}_2] / 10^{-4} \text{ M}$	before oscillation	1.76167	1.68693	1.59456	1.60643	1.4789
	at oscillation maximum	1.68488	1.55615	1.51382	1.48433	1.35996
$[\text{I}_3^-] / 10^{-7} \text{ M}$	before oscillation	2.5619	0.972281	0.469011	4.41456	4.86249
	at oscillation maximum	1.92716	1.34846	0.0958074	3.58152	2.12181
$[\text{Total iodine}] / 10^{-4} \text{ M}$	before oscillation	1.76423	1.68791	1.59503	1.61084	1.48376
	at oscillation maximum	1.68681	1.55749	1.51391	1.48791	1.36208
$\Delta[\text{Total iodine}] / 10^{-5} \text{ M}$		-0.774191	-1.3041	-0.811187	-1.22935	-1.21679
$\Delta[\text{Total iodine}]_{\text{aliquot}} / 10^{-5} \text{ M}$		-3.09676	-5.21642	-3.24475	-4.91739	-4.86715
$\Delta n(\text{Total iodine})_{\text{in 30 mL reaction mixture}} / 10^{-6} \text{ mol}$		-0.929029	-1.56492	-0.973424	-1.47522	-1.46015
Mean value of $\Delta n(\text{Total iodine})_{\text{in 30 mL reaction mixture}} / 10^{-6} \text{ mol}$		-1,28055				
Standard error of the mean $\Delta n(\text{Total iodine})_{\text{in 30 mL reaction mixture}} / 10^{-6} \text{ mol}$		0.135814				